PAPER • OPEN ACCESS

Characterization of mechanical properties and formability of a superplastic Al-Mg alloy

View the article online for updates and enhancements.

Related content

- Experimental and numerical investigation of strain rate effect on low cycle fatigue behaviour of AA 5754 alloy
  P Kumar and A Singh

- Optimization and selection of forming depth and pressure for box shaped Superplastic forming using grey based fuzzy logic
  Jalumedi Babu, Madarapu Anjaiah, Varkeychen et al.

- Properties and microstructure of twin-roll cast Al-Mg alloy containing Sc and Zr
  M Cieslar, J Bajer, M Zimina et al.

IOP ebooks™

Bringing you innovative digital publishing with leading voices to create your essential collection of books in STEM research.

Start exploring the collection - download the first chapter of every title for free.

Characterization of mechanical properties and formability of a superplastic Al-Mg alloy

Omid Majidi[1]**, Mohammad Jahazi**[1] **and Nicolas Bombardier**[2]

[1] Aluminium Research Centre-REGAL, Ecole de technologie superieure, Montreal, QC, H3C 1K3, Canada
[2] Verbom Inc., 3820 Boulevard Industriel, Sherbrooke, QC, J1L 2V1, Canada

E-mail: omid.majidi.1@ens.etsmtl.ca, mohammad.jahazi@etsmtl.ca, Nicolas.Bombardier@verbom.com

Abstract. In order to develop a reliable constitutive model for predicting formability and springback of sheet metals during superplastic forming (SPF) and quick plastic forming (QPF), characterization of elastic-plastic behavior, as well as formability of the material is essential. In the present study, the module of elasticity, uniaxial flow behavior and anisotropy, as well as the forming limit curve (FLC) of one of an SPF/QPF grade AA5083 was investigated. The variation of Young's modulus with temperature was measured from the uniaxial tensile tests for four temperatures ranging from 25 to 500 ºC. The impact of temperature and strain rate on the flow behavior of the material was investigated via uniaxial tensile tests for three temperatures (420, 450, and 480 ºC) and at three strain rates (0.001, 0.01, and 0.1 s^{-1}). The dependency of the flow stress on the material orientation with respect to the rolling direction (0, 45, and 90º) was assessed using uniaxial tensile tests at a constant temperature. In addition, the evolution of plastic anisotropy with plastic strain and strain rate was assessed by measuring the Lankford coefficient (r-value). Finally, the FLC of the material at 450 ºC was characterized according to Nakazima tests procedure for three strain paths (i.e. uniaxial tension, plane strain, and biaxial tension).

1. Introduction
It has been reported that aluminum alloys with fine grains (~ 10 μm), at elevated temperatures (over 0.5 of melting point) and low strain rates (less than 0.01 s^{-1}) show superior ductility, known as superplasticity [1-3]. Superplastic forming (SPF) and most recently hybrid superplastic forming, e.g. High-Speed Blow Forming (HSBF), have been introduced for manufacturing complex aluminum components [4].

In practice, SPF/HSBF processes are very sensitive to the applied strain rate (e.g., forming cycle) and temperature [2]. Finite element simulations have been used for tuning the process parameters in order to prevent excessive thinning as well as distortions of the parts. To this end, material constitutive modeling has a key role in the accuracy of the numerical simulations and it strongly relies on characterization of mechanical and formability behaviors.

Compared with conventional materials, superplastic metals are characterized at elevated temperatures. Thus, the main challenge for characterizing plastic anisotropy and forming limit diagrams (FLDs) for superplastic metals is conducting experiments at elevated temperatures.

Moreover, deformation mechanisms of superplastic metals differ from the ones for traditional alloys which make them very sensitive to strain rate changes [2-3]. The forming limit
The authors recently reported the dependency of the strain rate sensitivity index (m-value) on the applied testing method [5]. It has been also reported that the geometry of the specimen has a significant impact on the uniaxial tensile test results for superplastic sheet metals [6]. Therefore, new standards (e.g., ASTM E2448) have been introduced for determination of mechanical properties of superplastic metals.
Among aluminum alloys, 5000 series (e.g., AA5083) are the most used ones for SPF applications. Several researchers have independently reported various aspects of flow behavior and formability of AA5083 [7-9]. Yet, the plastic strain ratio (r-value) under superplastic conditions has not been reported for this alloy. Nevertheless, the applied methodologies, material grades, standards, and devices are variable in the literature which makes uncertainty for practical applications. Consequently, a comprehensive investigation on the characterization of elastic-plastic and anisotropic behavior as well as forming limits of superplastic Al-Mg alloy is essential which is the aim of the present manuscript.

2. Experimental procedures

In this study, four groups of experiments were performed on superplastic AA5083 specimens with an initial thickness of 1.2 mm. As summarized in Table 1, for assessing elastic modulus, isotropic hardening behavior, Lankford coefficient (r-value), and forming limit curve (FLC), several tests at different temperatures, strain rates, and materials orientations were carried out. Each test condition was repeated at least three times. All the tests were performed using an MTS machine equipped with a furnace. For uniaxial tension tests, depending on the test category, the specimens were prepared according to ASTM E8 or ASTM E2448 standards (see Figure 1).
For measuring elastic modulus, the ASTM E8 samples were used since it has a longer gauge length for attaching an extensometer. The tests were performed at four temperatures (i.e. 25, 350, 450, and 500 ºC). In order to eliminate the errors due to extensometer slipping during the initial loading, after certain preloads (tension) the samples were unloaded and reloaded again. The unloading-reloading were, then, considered for measuring Young's modulus (see Figure 2).

Table 1. Test conditions

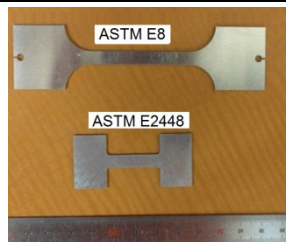| Category	Test method	Strain rate (s^{-1})	Temperature $(ºC)$	Sample Orientation wrt rolling direction
Elastic properties	Uniaxial tension (ASTM E8)	0.001	25, 350, 450, & 500	0
Isotropic hardening	Uniaxial tension (ASTM E2448)	0.001	420, 450 & 480	0
		0.001	450	90 and 45
		0.01 & 0.1	450	0
Plastic Anisotropy	Uniaxial tension (ASTM E8)	0.001, 0.01, & 0.1	450	0 (ε: 20%)
				90 (ε: 20%)
		0.01		45 (ε: 15, 20, 40%)
Forming Limit Curve (FLC)	Nakazima test	0.01	450	0 (Biaxial, plane strain, and uniaxial)

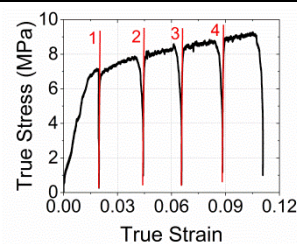**Figure 1.** The two specimen geometries used in this study.

Figure 2. The stress-strain curve for measuring elastic modulus for temperature of 500 ºC.

For assessing uniaxial tensile behaviors (isotropic hardening curves) it was not practicable to use the mechanical extensometers and, consequently, the crosshead displacements were used for measuring strains. As discussed in Ref. [10], the ASTM E2448 is recommended for this application. The uniaxial tensile tests were performed for three temperatures (420, 450, and 480 ºC) at a constant strain rate (0.001 s^{-1}). Furthermore, at a constant temperature of 470 ºC, the impact of strain rate and material orientation with respect to the rolling direction was investigated. In this study, plastic strain ratio (r-value) was determined from Eq.1 according to ASTM E517 methodology.

$$r = \frac{\varepsilon_w}{\varepsilon_t} = \frac{\ln(\frac{w_f}{w_0})}{\ln(\frac{t_f}{t_0})} \qquad (1)$$

where ε_w and ε_t are width and thickness strains, respectively and w_0, t_0 are the mean width and thickness of the specimen before deformation while the w_f and t_f are the mean width and thickness of the deformed parts. For each specimen, the initial and post-deformation width and thickness profiles were carefully measured along 20 mm of the gauge length using a coordinate-measuring machine (CMM) with a CNC machine.

Finally, the forming limit curve (FLC) of the studied material was measured using Nakazima punch test for three strain paths (i.e. near biaxial, near plane strain and near uniaxial). For this purpose, an in-house test set-up was used. In this set-up, the specimen was tightly clamped between the tools and was deformed by a punch with a spherical head (diameter: 101.7 mm). The punch motion was controlled to maintain a constant strain rate of ~0.01 s^{-1}. The tools and the specimen were located in the furnace to achieve a constant temperature ~ 450 ºC.

To measure the amount of strain experienced by a sample, according to ASTM 2218 standard, an etched-on grid pattern (1x1 mm) was applied on the surface of each specimen. The initial and the final thickness of the deformed parts were measured using a CMM machine. Also, the grid patterns were carefully recorded by a Mitutoyo® micrometer before and after the tests to calculate the major and minor in-plane strains. In the present work, rather than at the crack location, the stretched gridded areas right near (above and below) a crack were considered. In order to minimize the effects of friction between the sheet sample and the tools, a graphite powder was applied on the surface of specimens before running each test.

3. Results and discussions:

3.1. *Young's modulus:*

As shown in Figure 3, increasing temperature reduces Young's modulus. In other words, by increasing temperature from 25 to 500 ºC, Young's modulus decreased by ~80%. Consequently, for assessing thermal distortion of superplastic metals, corresponding Young's modulus should be considered in numerical simulations. Similar result could be seen for AA5083 in Ref. [10]. As shown in Fig. 3, by a cubic interpolation (dashed line) the experimental data were fitted, where the rate of changes for Young's modulus is comparatively smooth at low (<150 ºC) and high (over 450 ºC) temperature ranges, compared with the intermediate temperatures.
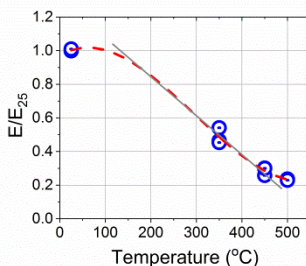

Figure 3. Variation of relative elastic modulus with temperature

3.2. Uniaxial flow behavior:

The uniaxial flow behavior of the material as a function of strain rate, temperature, and orientation of the specimen with respect to the rolling direction is presented in Figure 4. As shown in this figure, material flow behavior strongly depends on the applied temperature and strain rate, while the impact of material orientation is negligible. For instance, by increasing strain rate from 10^{-3} to 10^{-2} s^{-1}, yield stress increases by 86%.
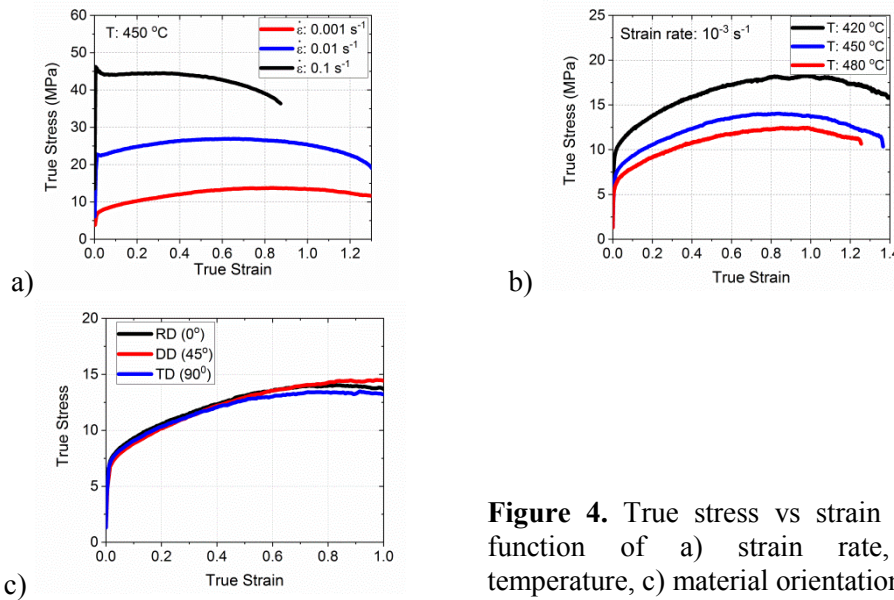

a)

b)

c)

Figure 4. True stress vs strain as a function of a) strain rate, b) temperature, c) material orientation.

To quantify the isotropic hardening behavior of the material, the plastic stress-strain curves were approximated by Voce model [12]:

$$\sigma = \sigma_s - (\sigma_s - \sigma_i)\exp(-\eta\varepsilon) \qquad (2)$$

where σ_i, σ_s, and η are initial plastic stress, saturation plastic stress, the rate of transient from the initial to saturation stress, respectively. The material parameters for different test conditions, determined by fitting the curves up 0.6 plastic strains, are presented in Table 2.

In this table, index H is considered as the hardening capacity and defined as:

$$H = \frac{(\sigma_s - \sigma_i)}{\sigma_i} \qquad (3)$$

Table 2. Voce hardening parameters for various test conditions

Strain rate (s^{-1})	Temperature (ºC)	Orientation (wrt RD)	σ_i (MPa)	σ_s (MPa)	η	H
	420	0	9.7	18.52	3.07	0.91
	480	0	6.1	12.8	3.04	1.10
0.001	450	0	7.1	14.83	3.06	1.09
	450	45	6.9	15.25	2.54	1.21
	450	90	7.1	14.9	3.04	1.10
0.01	450	0	21.5	27.78	4.26	0.29
0.1	450	0	43.5	44.27	8.44	0.02

According to Figure 4 and Table 2, compared with temperature and material orientation, strain rate has the most impact on the variation of the initial stress, hardening capacity and the rate of hardening evolution. For instance, by increasing strain rate from 0.001 to 0.1 s^{-1}, the initial stress increases significantly, and hardening capacity drops to near zero. However, both parameters remain almost

constant by changing the material orientation. The temperature variation has a noticeable impact on the initial stress, but it does not alter the material hardening pattern.

3.3. *Plastic anisotropy:*

The dependency of r-value on the strain rate, plastic strain, and material orientation is presented in Figure 5. For the same material orientation (rolling direction) and at a constant plastic strain (20%), when strain rate increases from 0.001 to 0.1 s^{-1}, the relative r-value grows by 6%. On the other hand, under a constant strain rate and material orientation, by increasing plastic strain from 15% to 40%, the r-value decreases by 11.4%. Finally, at a constant strain rate and plastic strain, the maximum normalized r-values is observed when the material orientation was 45 with respect to the rolling direction. Overall, the r-value is near unity and the material planar anisotropy, calculated from Eq. 4, is about 0.04 which is negligible.
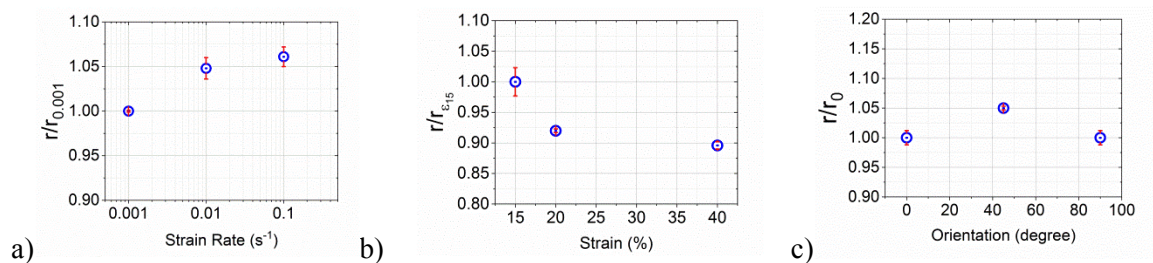
$$r_p = \frac{r_0 - 2r_{45} + r_{90}}{2}$$

(4)

Figure 5. Variation of relative r-values with a) strain rate, b) plastic strain, c) the material orientation.

3.4. *Forming Limit Curve (FLC):*

The three representative specimens and the calculated forming limit curve of the studied material are presented in Figure 6. As expected, up to a high level of strains (an equivalent plastic strain of ~1.5), the material was deformed safely. According to this curve, the minimum formability is observed for the near biaxial tension stress state, which follows the same trends observed by other researchers [7, 9]. Nonetheless, this observation differs from the ones for the conventional sheet metals at the ambient temperature, where a minimum formability usually occurs at near plane strain condition. This could be explained by the governing deformation and damage mechanisms of superplastic metals. Under superplastic conditions (i.e. elevated temperature, fine grain size, and low strain rate), grain boundary sliding is likely the main deformation mechanism [2-3]. On the other hand, the damage mechanism of superplastic metals is attributed to the formation and growth of cavities in the grain boundaries where the evolution of cavitation strongly depends on the stress triaxiality [13]. Thus, compared with other strain paths, the highest rate of cavitation is expected for biaxial tension, which eventually degrades the forming limit.

Figure 6. a) The deformed specimens, b) Forming Limit Curve (T: 450 ºC, strain rate: 0.01 s^{-1})

4. Conclusions

The uniaxial elastic-plastic behavior of an AA5083 sheet alloy was investigated and the following behaviors were observed:

- The variation of Young's modulus with temperature was observed in this study which could be implemented to further increase the accuracy of simulations.
- Although the impact of temperature and strain rate on flow behavior of superplastic metals is well-documented in literature, in the present study the three most important parameters (e.g., temperature, strain rate and plastic anisotropy) were investigated, comparatively. It was found that among the three variables, the strain rate has the highest impact on plastic yield stress and hardening behavior. Temperature variation alters the yield stress, but it does not change the isotropic hardening behavior, significantly. The impact of material orientation on the uniaxial flow behavior was negligible.
- The r-value has less been investigated for the studied material in literature. According to this study, it was found the material anisotropy index (r-value) is mostly near unity. The r-value slightly increases with strain rate and decreases with plastic strain. For the studied material, the planar anisotropy is negligible.
- According to FLC curve, compared with plane strain and uniaxial tension, formability of the studied material is less under biaxial tension mode. The same bahvior has been reported for SPF metals.

References

[1]   Otsuka M and Horiuchi R 1977 *J. Japan Inst. Light Met.* **27** 85
[2]   Langdon T G 1982 *Metall. Trans. A* **13** 689
[3]   Kulas M A, Green W P, Taleff E M, Krajewski P E and McNelley T R 2005 *Metal. Mater. Trans. A*, **36** 1249
[4]   Krajewski P E, Schroth J G 2007 *Mater. Sci. Forum* **551** 3
[5]   Majidi O, Jahazi M, Bombardier N and Samuel E 2017 *AIP Conf. Proc.* **1896** 020022
[6]   Abu-Farha F K and Khraisheh M K 2007 *J. Mater. Eng. Perform.* **16** 142
[7]   Banabic D, Vulcan M and Siegert K 2005 *CIRP Annals-Manuf. Technol.* **54** 205
[8]   Mitukiewicz G, Anantheshwara K, Zhou G, Mishra R K and Jain M K 2014 *J. Mater. Process. Technol.* **214** 2960
[9]   Yogesha B, Divya H V and Bhattacharya S S 2014 *Adv. Mater. Res.* **902** 1829
[10] Summers P T et al. 2015 *Fire Sci. Rev.* **4** 3
[11] Comley P N 2008 *J. Mater. Eng. Perform.* **17** 183
[12] Voce E 1955 A practical strain hardening function *Metallurgia* **51** 219
[13] Bae D H, Ghosh A K and Bradley J R 2003 *Metall. Mater. Trans. A* **34** 2449